Contribution from the Department of Chemistry,
University of Minnesota, Minneapolis, Minnesota 55455

Electrophilic Attack on a Cluster-Coordinated Nitrosyl Ligand: Crystal and Molecular Structure of $Ru_3(NOCH_3)(CO)_{10}$ and Observation of an O-H to M-H Tautomerization

Robert E. Stevens, Robert D. Guettler, and Wayne L. Gladfelter*

Received February 22, 1989

The reactions of the anionic cluster $[Ru_3(CO)_{10}(NO)]^-$ with acids and $CF_3SO_3CH_3$ are reported. O-Methylation of the μ_2-NO ligand gives high yields of $Ru_3(NOCH_3)(CO)_{10}$. A single-crystal X-ray crystallographic analysis of this new cluster [orthorhombic crystal system, *Pnma* space group, a = 14.775 (4) Å, b = 12.128 (2) Å, c = 9.987 (2) Å, Z = 4] revealed the presence of a triply bridging methoxyimido ($NOCH_3$) ligand and a triply bridging carbonyl ligand on opposite faces of an equilateral ruthenium triangle. O-Protonation with CF_3SO_3H gives an analogous structure; however, weaker acids, such as CF_3CO_2H, give only $HRu_3(CO)_{10}(NO)$, where a Ru-Ru bond has been protonated. Addition of $PPN(CF_3CO_2)$ to $Ru_3(NOH)(CO)_{10}$ results in immediate O-H to M-H tautomerization. The PPN^+ salts of 12 anions having differing basicities provide insight into the pK_a of $Ru_3(NOH)(CO)_{10}$ and the relative kinetic acidity of the O-H vs the M-H group. Reactions of the substituted anions $[Ru_3(CO)_9(L)(NO)]^-$, where L = PPh_3 and $P(OCH_3)_3$, with acids reveal similar behavior.

Introduction

Studies of electrophilic attack on coordinated nitric oxide have, until recently, been limited to mononuclear metal complexes.[1,2] Several of these studies involving the reaction of protons with various M-NO groups have resulted in products containing a new N-H bond.[3-8] For instance, the reaction of HCl with $OsCl(CO)(PPh_3)_2(NO)$ (eq 1) gives a species containing a nitrosyl

$$OsCl(CO)(PPh_3)_2(NO) + HCl \rightarrow OsCl_2(CO)(PPh_3)_2(HNO) \quad (1)$$

hydride, HNO,[4] which has been structurally characterized.[5] In the case of $Os(PPh_3)_3(NO)$, further reaction occurs to give an NHOH ligand,[4] while the NO in $Rh(PPh_3)_3(NO)$ yields free hydroxylamine.[6,7] In other cases the protonation product has been postulated to be an NOH ligand, as in $[Fe(CN)_5(NOH)]^{2-}$[9,10] and $RhCl_3(NOH)(PPh_3)$,[6] although in no case has any direct, unequivocal evidence for such a species been presented.

In contrast to the extensive reactivity studies of NO on mononuclear complexes, few studies exist on the chemistry of metal-cluster-coordinated nitric oxide. This has mainly been due to the lack of a general synthetic method for the preparation of such species. The discovery that $PPN(NO_2)$ can be used to generate carbonyl nitrosyl clusters[11] has provided the opportunity to explore this reactivity. Metal clusters allow the nitrosyl ligand to bridge either two metal atoms, as in $[Ru_3(CO)_{10}(NO)]^-$ and $[Os_3(CO)_{10}(NO)]^-$,[12] or three metal atoms, as in $Cp_3Mn_3(NO)_4$.[13] For both binding modes, the oxygen of the bridging ligand is more susceptible to electrophilic attack due to increased back-bonding and the resultant reduction of the N-O bond order. Similar arguments have led to a large number of O-alkylations and -protonations of bridging carbonyl ligands.[14-32] In the preliminary report of this work,[33] we described the O-methylation and O-protonation of $[Ru_3(CO)_{10}(NO)]^-$. Since then, the O-protonation of $MeCp_3Mn_3(NO)_4$ has been reported,[34] including the X-ray structural analysis confirming the N-O-H linkage (I). O-Protonation of $[CpWFe_2(CR)(CO)_7(NO)]^-$ has also been reported to yield the μ_3-NOH ligand.[35]

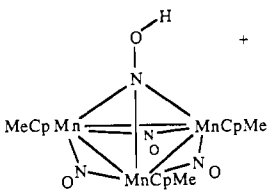

I

Experimental Section

$PPN(Cl)$,[36] $PPN(Br)$,[37] $PPN(I)$,[37] $PPN(NO_3)$,[37] $PPN(ClO_4)$,[37] and $PPN[Ru_3(CO)_{10}(NO)]$[11] [PPN = bis(triphenylphosphine)nitrogen(1+)]

(1) Richter-Addo, G. B.; Legzdins, P. *Chem. Rev.* **1988**, *88*, 991.
(2) McCleverty, J. A. *Chem. Rev.* **1979**, *79*, 53.
(3) Enemark, J. H.; Feltham, R. D.; Riker-Nappier, J.; Bizot, K. F. *Inorg. Chem.* **1975**, *14*, 624.
(4) Grundy, K. R.; Reed, C. A.; Roper, W. R. *J. Chem. Soc., Chem. Commun.* **1970**, 1501.
(5) Wilson, R. D.; Ibers, J. A. *Inorg. Chem.* **1979**, *18*, 336.
(6) Collman, J. P.; Hoffman, N. W.; Morris, D. E. *J. Am. Chem. Soc.* **1969**, *91*, 5659.
(7) Dolcetti, G.; Hoffman, N. W.; Collman, J. P. *Inorg. Chim. Acta* **1972**, *6*, 531.
(8) LaMonica, G.; Freni, M.; Cenini, S. *J. Organomet. Chem.* **1974**, *71*, 57.
(9) van Voorst, J. D. W.; Hemmerich, P. *J. Chem. Phys.* **1966**, *45*, 3914.
(10) Nast, R.; Schmidt, J. *Angew. Chem., Int. Ed. Engl.* **1969**, *8*, 383.
(11) Stevens, R. E.; Gladfelter, W. L. *Inorg. Chem.* **1983**, *22*, 2034.
(12) Johnson, B. F. G.; Lewis, J.; Mace, J. M.; Raithby, P. R.; Stevens, R. E.; Gladfelter, W. L. *Inorg. Chem.* **1984**, *23*, 1600.
(13) Elder, R. C. *Inorg. Chem.* **1974**, *13*, 1037.
(14) Shriver, D. F.; Lehman, D.; Strope, D. *J. Am. Chem. Soc.* **1975**, *97*, 1594.
(15) Gavens, P. D.; Mays, M. J. *J. Organomet. Chem.* **1978**, *162*, 389.
(16) Keister, J. B. *J. Chem. Soc., Chem. Commun.* **1979**, 214.
(17) Johnson, B. F. G.; Lewis, J.; Orpen, A. G.; Raithby, P. R.; Suss, G. *J. Organomet. Chem.* **1979**, *173*, 187.
(18) Holt, E. M.; Whitmire, K.; Shriver, D. F. *J. Chem. Soc., Chem. Commun.* **1980**, 778.
(19) Whitmire, K.; Shriver, D. F.; Holt, E. M. *J. Chem. Soc., Chem. Commun.* **1980**, 780.
(20) Dawson, P. A.; Johnson, B. F. G.; Lewis, J.; Raithby, P. R. *J. Chem. Soc., Chem. Commun.* **1980**, 781.
(21) Hodali, H. A.; Shriver, D. F.; Ammlung, C. A. *J. Am. Chem. Soc.* **1978**, *100*, 5239.
(22) Fachinetti, G. *J. Chem. Soc., Chem. Commun.* **1979**, 397.
(23) Keister, J. B. *J. Organomet. Chem.* **1980**, *190*, C36.
(24) Whitmire, K. H.; Shriver, D. F. *J. Am. Chem. Soc.* **1981**, *103*, 6754.
(25) Churchill, M. R.; Beanan, L. R.; Wasserman, H. J.; Bueno, C.; Rahman, Z. A.; Keister, J. B. *Organometallics* **1983**, *2*, 1179.
(26) Keister, J. B.; Payne, M. W.; Muscatella, M. J. *Organometallics* **1983**, *2*, 219.
(27) Pribich, D. C.; Rosenberg, E. *Organometallics* **1988**, *7*, 1741.
(28) Wong, W.-K.; Chiu, K. W.; Wilkinson, G.; Galas, A. M. R.; Thornton-Pett, M.; Hursthouse, M. B. *J. Chem. Soc., Dalton Trans.* **1983**, 1557.
(29) Farrugia, L. J. *J. Organomet. Chem.* **1986**, *310*, 67.
(30) Aitchison, A. A.; Farrugia, L. J. *Organometallics* **1986**, *5*, 1103.
(31) Farrugia, L. J. *J. Chem. Soc., Chem. Commun.* **1987**, 147.
(32) Green, M.; Mead, K. A.; Mills, R. M.; Salter, I. D.; Stone, F. G. A.; Woodward, P. *J. Chem. Soc., Chem. Commun.* **1982**, 51.
(33) Stevens, R. E.; Gladfelter, W. L. *J. Am. Chem. Soc.* **1982**, *104*, 6454.
(34) Legzdins, P.; Nurse, C. R.; Rettig, S. J. *J. Am. Chem. Soc.* **1983**, *105*, 3727.
(35) Delgado, E.; Jeffery, J. C.; Simmons, N. D.; Stone, F. G. A. *J. Chem. Soc., Dalton Trans.* **1986**, 869.
(36) Ruff, J. K.; Schlientz, W. J. *Inorg. Synth.* **1974**, *15*, 84.
(37) Martinsen, A.; Songstad, J. *Acta Chem. Scand.* **1977**, *A31*, 645.
(38) Levy, G. C.; Lichter, R. L. *Nitrogen-15 Nuclear Magnetic Resonance Spectroscopy*; Wiley: New York, 1979.

0020-1669/90/1329-0451$02.50/0

Table I. Spectroscopic Data

compd	ν_{CO}, cm^{-1}	ν_{NO}, cm^{-1}	CD_2Cl_2 ^1H NMR, ppm	CD_2Cl_2 ^{31}P NMR, ppm
$PPN[Ru_3(CO)_{10}(NO)]$	2069 w, 2010 s, 2001 vs, 1971 s, 1945 m (THF)	1479 ($CHCl_3$)	none[a]	none[a]
$Ru_3(NOCH_3)(CO)_{10}$	2106 w, 2069 vs, 2032 vs, 2026 m, 2017 s, 1745 m (hexane)	945 (KBr)	3.45($J_{^{15}N-^1H}$ = 4.4 Hz)	none
$Ru_3(NOH)(CO)_{10}$	2101 vw, 2070 vs, 2032 s, 2015 m, 1744 m (hexane)	1110 (CH_2Cl_2)	8.90	none
$Ru_3(NOH)(CO)_9[P(OMe)_3]$	2092 w, 2061 s, 2046 vs, 2023 s, 1729 w (hexane)	*b*	9.32 (s, 1 H), 3.76 (d, J_{P-H} = 12.1 Hz, 9 H)	147.4
$HRu_3(CO)_{10}(NO)$[c]	2109 w, 2070 vs, 2064 s, 2033 vs, 2027 m, 2019 s, 1998 w	1550 w	−11.85	
$HRu_3(CO)_9[P(OMe)_3](NO)$	2096 m, 2057 vs, 2023 vs, 2004 s, br 1990 m (hexane)	1524 w	3.61 (d, J_{P-H} = 12.5, 9 H), −12.10 (d, J_{P-H}) = 8.1 Hz, 1 H)	135.8
$Ru_3(NOH)(CO)_9(PPh_3)$	2088 w, 2074 m, 2061 s, 2025 vs, 1960 w, 1718 w (hexane)	*b*	8.80 (s, 1 H), 7.4 (m, 15 H)	46.0
$HRu_3(CO)_9(PPh_3)(NO)$	2094 m, 2056 s, 2021 vs, 2002 m, 1991 w (hexane)	*b*	7.37 (m, 15 H) −11.44 (d, J_{P-H} = 6.7 Hz, 1 H)	33.8

[a] Excluding PPN cation resonances. [b] Not observed. [c] Reference 40.

were prepared according to published procedures. All of the ^{15}N-enriched compounds were prepared from $PPN(^{15}NO_2)$ as described elsewhere.[11] CF_3SO_3H, $CF_3SO_3CH_3$, FSO_3H, CF_3CO_2H, $P(OCH_3)_3$, and $P(C_6H_5)_3$ were purchased from Aldrich Chemical Co. and used without purification. Methylene chloride was dried by distillation from P_2O_5 under vacuum. Hexane was dried by distillation from sodium under nitrogen. Diethyl ether was dried by distillation from sodium benzophenone ketyl under nitrogen. Reagent grade acetone was used without purification. All reactions, with the exception of the syntheses of the PPN^+ salts, were carried out under a nitrogen atmosphere that was maintained up to the point of hexane extraction of the neutral products. Chromatography was conducted on silica gel. Infrared spectra were recorded on a Beckman 4250 spectrophotometer, and the ^1H NMR spectra were obtained on a Varian CFT20 80-MHz spectrophotometer. The ^{31}P NMR data were obtained on a Nicolet NTCFT-1180 300-MHz spectrophotometer, and the chemical shifts are reported relative to H_3PO_4. ^{15}N NMR spectra were also obtained on a Nicolet NTCFT-1180 300-MHz spectrophotometer using 90% enriched samples. Each ^{15}N NMR spectrum was obtained with use of a 12-mm tube and CH_2Cl_2 (~3.5 mL) as a solvent. Sample concentrations of approximately 0.03 M were used, and $Cr(acac)_3$ (53 mg) was added as a shiftless relaxation reagent. External referencing was done with CH_3NO_2 in $CHCl_3$ containing 0.03 M $Cr(acac)_3$ set at 379.60 ppm downfield from NH_3 (liquid, 25 °C).[30] All data are reported relative to NH_3. Spectroscopic data are presented in Table I.

Preparation of $Ru_3(NOCH_3)(CO)_{10}$. $CF_3SO_3CH_3$ (121 μL, 1.07 mmol) was added slowly to a solution of $PPN[Ru_3(CO)_{10}(NO)]$ (865.5 mg, 0.751 mmol) in methylene chloride at room temperature. The reaction mixture was stirred for 40 min, during which time the color changed from deep yellow-green to bright gold. The volume was reduced under vacuum to 10 mL, and diethyl ether (60 mL) was added via syringe. The resulting cream-colored precipitate, principally $PPN(CF_3SO_3)$, was filtered from the gold solution, washed with diethyl ether (2 × 10 mL), and discarded. The gold diethyl ether solution was evaporated under vacuum, and the residue was extracted with hexane to give a bright lemon yellow solution. Chromatography of the solution gave two bands. The first band was yellow and contained a minor amount of $Ru_3(CO)_{12}$. From the second band, which was bright lemon yellow, the major product, $Ru_3(NOCH_3)(CO)_{10}$ (406.6 mg, 0.647 mmol), was obtained in 86% yield. Mass spectrum: m/z 602 (parent not observed), followed by 10 peaks each corresponding to a loss of carbon monoxide. Anal. Calcd for $Ru_3O_{11}NC_{11}H_3$: C, 21.03; H, 0.48; N, 2.23. Found: C, 21.44; H, 0.49; N, 2.11.

Preparation of $Ru_3(NOH)(CO)_{10}$. $PPN[Ru_3(CO)_{10}(NO)]$ (123.7 mg, 0.107 mmol) was placed in a Schlenk tube and degassed. Freshly distilled CH_2Cl_2 (15 mL) was added via syringe, and the resulting yellow-green solution was cooled to −78 °C with a dry ice/2-propanol bath. CF_3SO_3H (11.0 μL, 0.124 mmol) was added via microsyringe, causing an immediate color change to lemon yellow upon mixing. After the reaction mixture was allowed to warm to room temperature, the volume of the solution was reduced under vacuum to ~2 mL and diethyl ether (25 mL) was added, causing precipitation of a creamy white crystalline solid from the yellow solution. The mixture was filtered, and the residue was washed with diethyl ether (2 × 5 mL). The white solid was identified as $PPN(CF_3SO_3)$ (63.1 mg, 0.092 mmol) and recovered in 86% yield.

Table II. Melting Points and Analytical Data for New PPN^+ Salts

X^-[a]	mp, °C	calc (found)
(FSO_3^-)	259–260	C, 67.81 (68.01); H, 4.74 (4.88); N, 2.19 (2.12)
$(CF_3SO_3)^-$	216–217	C, 64.62 (64.57); H, 4.40 (4.38); N, 2.04 (1.98)
$(CF_3CO_2)^-$	190–191	C, 70.04 (69.82); H, 4.64 (4.86); N, 2.15 (2.09)
$(p\text{-tolSO}_3)^-$	177–178	C, 72.77 (72.21); H, 5.25 (5.41); N, 1.97 (1.93)
Cl_2pic^-	150–151	C, 60.37 (60.41); H, 3.74 (3.74); N, 6.71 (6.58)
pic^-	144–145	C, 65.79 (65.94); H, 4.20 (4.23); N, 7.30 (7.40)

[a] *p*-tol = toluene; pic = picrate.

The solvent was removed from the yellow solution under vacuum to give a yellow-brown oil. The oil was extracted and filtered with hexane (3 × 8 mL) to give a bright lemon yellow solution and a brown oil. Removal of the hexane under vacuum gave a lemon yellow oil that turns brown upon standing (~1 h) at either room temperature or −78 °C. The brown oil is insoluble in hexane.

Preparation of $Ru_3(NOH)(CO)_9[P(OCH_3)_3]$. $PPN[Ru_3(CO)_{10}(NO)]$ (96.7 mg, 0.084 mmol) was placed in a Schlenk tube, degassed, and dissolved in CH_2Cl_2 (5 mL). A solution of $P(OCH_3)_3$ (10.0 μL, 0.080 mmol) in CH_2Cl_2 (10 mL) was added dropwise to the ruthenium solution. Infrared spectroscopy showed conversion to $[Ru_3(CO)_9(P(OCH_3)_3)(NO)]^-$.[39] The volume was reduced under vacuum to ~8 mL, and the orange solution was frozen with liquid nitrogen. The reaction mixture was allowed to warm to room temperature after addition of CF_3SO_3H (7.5 μL, 0.085 mmol) via microsyringe. As the solution formed, it became light yellow, and infrared spectroscopy showed the presence of a triply bridging carbonyl peak at 1710 cm^{-1}. The volume was reduced under vacuum to ~1 mL, and diethyl ether (15 mL) was added, precipitating $PPN(CF_3CO_2)$. The yellow solution was filtered, and the precipitate was washed with diethyl ether (2 × 3 mL). The solvent was removed under vacuum, the residue was extracted with hexane (3 × 10 mL), and the resulting mixture was filtered to give a bright yellow solution. Removal of the solvent under vacuum gave a yellow oil that turned brown upon standing under nitrogen at room temperature. The brown oil is insoluble in hexane.

Formation of $Ru_3(NOH)(CO)_9(PPh_3)$. $PPN[Ru_3(CO)_{10}(NO)]$ (111.1 mg, 0.111 mmol) was placed in a Schlenk tube, degassed, and dissolved in CH_2Cl_2 (8 mL). PPh_3 (11.1 mg, 0.111 mmol) was dissolved in CH_2Cl_2 (10 mL), and the mixture was added dropwise to the $PPN[Ru_3(CO)_{10}(NO)]$ solution over a 20-min period. Infrared spectroscopy showed the presence of $[Ru_3(CO)_9(PPh_3)(NO)]^-$.[39] The volume was reduced to ~8 mL under vacuum, and the solution was cooled to −78 °C. CF_3SO_3H (11.1 μL, 0.111 mmol) was added via microsyringe, and the solution turned light orange with mixing. The reaction mixture was allowed to warm to room temperature, and the solvent was removed under vacuum. The residue was extracted with diethyl ether (2 × 10 mL) and the mixture was filtered to give an orange solution. The ether was removed under vacuum to give an orange oil that was not soluble in hexane.

Preparation of PPN(X) (X = ClO_4, CF_3SO_3, FSO_3, I, Br, *p*-Toluenesulfonate, Dichloropicrate, and Picrate). PPN(Cl) (1.0 g, 1.7

(39) Stevens, R. E.; Fjare, D. E.; Gladfelter, W. L. *J. Organomet. Chem.* **1988**, *347*, 373.

Table III. Results of Tautomerization Experiments: pK_a's of Conjugate Acids in Acetonitrile

salt	tautomerizn	pK_a(HX)	salt	tautomerizn	pK_a(HX)
PPN(ClO_4)	no	1.6[a]	PPN(Cl_2pic)	yes	8.12[c]
PPN(CF_3SO_3)	no	2.6[a]	PPN(Cl)	yes	10.4[b]
PPN(FSO_3)	no	3.4[a]	PPN(NO_3)	yes	10.5[b]
PPN(I)	yes		PPN(pic)	yes	11.0[b]
PPN(Br)	yes	5.8[b]	PPN(CF_3CO_2)	yes	~15[d]
PPN(*p*-tolSO_3)	yes	8.0[a]	PPN(NO_2)	yes	

[a] Reference 51. [b] Reference 52. [c] Reference 53. [d] Estimated from the pK_a of CH_3CO_2H in CH_3CN (22.3)[52] and the ΔpK_a in CH_3CN of 7.4 between CF_3SO_3H and CH_3SO_3H.[51]

mmol) was dissolved in distilled water (40 mL) at ~60 °C. The resulting solution was added dropwise with rapid mixing to a warm (~60 °C) solution of a 20-fold excess of NaX or KX (prepared by either dissolution of the appropriate salt or titration of a solution of HX with NaOH to pH = 6–8) in distilled water (60 mL). Immediate precipitation of a crystalline solid was observed, and the mixture was allowed to cool to room temperature. The solution was removed by filtration, and the precipitate was air-dried. The product was recrystallized from acetone/diethyl ether to a constant melting point and air-dried. The yields, elemental analyses, and melting points of the salts are presented in Table II.

Tautomerization Reactions. In a typical experiment, PPN[$Ru_3(CO)_{10}(NO)$] (60.4 mg, 0.052 mmol) was placed in a Schlenk tube and degassed. Freshly distilled CH_2Cl_2 (10 mL) was added via syringe, and the solution was cooled to −78 °C in a dry ice/2-propanol bath. CF_3SO_3H (5.0 μL, 0.056 mmol) was added via microsyringe, causing formation of $Ru_3(CO)_{10}(NOH)$ upon mixing. The solution was allowed to warm to room temperature, and the volume was reduced to ~2 mL under vacuum. Addition of diethyl ether (15 mL) caused precipitation of PPN(CF_3SO_3). The mixture was filtered, and the residue was washed with diethyl ether (5 mL). The solvent was removed under vacuum to give a yellow oil. The oil was dissolved in CH_2Cl_2 (5 mL), and infrared spectroscopy of the bright yellow solution showed the presence of only $Ru_3(NOH)(CO)_{10}$. PPN(X), approximately 0.50 equiv, was placed in a Schlenk tube and degassed. The methylene chloride solution of $Ru_3(CO)_{10}(NOH)$ was transferred via a cannula onto the PPN(X) with rapid stirring. Infrared spectroscopy as well as color changes was used to determine whether or not tautomerization occurred. $HRu_3(CO)_{10}(NO)$ was identified by its infrared spectrum[40] and by the color change from lemon yellow for $Ru_3(CO)_{10}(NOH)$ to orange-red for $HRu_3(CO)_{10}(NO)$. The results of these experiments are listed in Table III.

Tautomerization of $Ru_3(NOH)(CO)_9[P(OCH_3)_3]$ to $HRu_3(CO)_9[P(OCH_3)_3](NO)$. PPN[$Ru_3(CO)_{10}(NO)$] (73.6 mg, 0.064 mmol) was placed in a Schlenk tube, degassed, and dissolved in CH_2Cl_2 (10 mL) in a pressure-equalizing addition funnel. The $P(OCH_3)_3$ solution was added dropwise to the PPN[$Ru_3(CO)_{10}(NO)$] solution over a 1-h period. Infrared spectroscopy at this point showed the presence of $[Ru_3(CO)_9(P(OCH_3)_3(NO)]^-$.[39] The solution was cooled to −78 °C with a dry ice/2-propanol bath, and CF_3SO_3H (6.0 μL, 0.068 mmol) was added via microsyringe. The cold bath was removed, and the reaction mixture was allowed to warm to room temperature. As the solution warmed, the color changed from deep red-orange to bright yellow, and infrared spectroscopy showed the presence of $Ru_3(NOH)(CO)_9[P(OCH_3)_3]$ by the presence of the triply bridging carbonyl absorbance at 1720 cm^{-1}. PPN(CF_3CO_2) (24.0 mg, 0.37 mmol) was placed in a Schlenk tube and degassed. The yellow $Ru_3(NOH)(CO)_9[P(OCH_3)_3]$ solution was transferred via a cannula onto the PPN(CF_3CO_2) with rapid stirring. The solution slowly turned orange-red as the reaction was monitored by infrared spectroscopy. After 2 h the tautomerization was complete as evidenced by the disappearance of the 1720-cm^{-1} band and the appearance of bands at 2095 and 1525 cm^{-1} for $HRu_3(CO)_9[P(OCH_3)_3](NO)$. The solvent was removed under vacuum, and the residue was extracted with hexane/CH_2Cl_2 (7/3) and chromatographed to give two bands. The first red band was identified by its infrared spectrum[31] as $HRu_3(CO)_{10}(NO)$ (14.0 mg, 0.023 mmol), 36% yield. The second orange band gave $HRu_3(CO)_9[P(OCH_3)_3](NO)$ (10.2 mg, 0.014 mmol) in 22% overall yield. This compound was also identified by its infrared spectrum.[40]

Collection and Refinement of the X-ray Data. Yellow crystals of $Ru_3(NOCH_3)(CO)_{10}$ were grown by slow cooling of a hexane solution of the cluster. A preliminary peak search indicated the crystal was orthorhombic, and the systematic absences ($hk0$, $h = 2n + 1$; $0kl$, $k + l = 2n + 1$) were consistent with the space groups *Pnma* or $Pn2_1a$. (The latter is a nonstandard setting of $Pna2_1$ corresponding to the axes as assigned here.) Successful refinement of the structure in the centric space group justified its assignment. A summary of the crystal data is presented in Table IV, and further details are similar to previous structural studies examined in our laboratory.[11] Three reflections monitored approximately every 120 reflections showed no significant decay throughout the entire data collection. The largest peak in the difference Fourier synthesis, after refinement of all the non-hydrogen atoms with anisotropic thermal parameters, appeared in the mirror plane near the methyl carbon

(40) Johnson, B. F. G.; Raithby, P. R.; Zuccaro, C. *J. Chem. Soc., Dalton Trans.* **1980**, 99.

Table IV. Summary of Crystallographic Data

formula	$Ru_3O_{11}N_1C_{11}H_3$	Z	4
fw	626.36	ρ(calcd), g cm^{-3}	2.332
space group	*Pnma*	temp, °C	23
a, Å	14.775 (4)	μ, cm^{-1}	24.95
b, Å	12.128 (2)	R	0.025
c, Å	9.987 (2)	R_w	0.035
V, Å^3	1790 (1)		

Table V. Positional Parameters

atom	x	y	z
Ru1	0.06901 (2)	0.13706 (3)	−0.23857 (3)
Ru2	0.17594 (3)	0.25000 (0)	−0.05784 (4)
O	0.2528 (3)	0.2500 (0)	−0.3312 (4)
O10	−0.0276 (3)	0.2500 (0)	0.0023 (4)
O11	0.0133 (3)	0.1213 (3)	−0.5325 (3)
O12	−0.1762 (3)	0.0783 (3)	−0.7724 (5)
O13	−0.1039 (3)	0.0191 (3)	−0.1452 (5)
O21	0.3117 (2)	0.0603 (4)	−0.0405 (4)
O22	0.1356 (5)	0.2500 (0)	0.2433 (5)
N	0.1692 (3)	0.2500 (0)	−0.2584 (4)
C	0.2390 (5)	0.2500 (0)	−0.4690 (7)
C10	0.0310 (4)	0.2500 (0)	−0.0772 (6)
C11	0.0326 (3)	0.1266 (3)	−0.4232 (4)
C12	0.1393 (4)	0.4984 (4)	−0.2301 (5)
C13	−0.0392 (3)	0.0608 (4)	−0.1814 (5)
C21	0.2618 (3)	0.1314 (5)	−0.0425 (5)
C22	0.1511 (5)	0.2500 (0)	0.1325 (6)

Table VI. Bond Distances (Å)

Ru1–Ru1′	2.740 (1)	Ru2–C10	2.150 (5)
Ru1–Ru2	2.762 (1)	N–O	1.433 (6)
Ru1–N	2.027 (3)	O–C	1.391 (8)
Ru2–N	2.006 (4)	C10–O10	1.175 (6)
Ru1–C10	2.188 (4)	C11–O11	1.130 (5)
Ru1–C11	1.925 (5)	C12–O12	1.112 (6)
Ru1–C12	1.945 (5)	C13–O13	1.140 (6)
Ru1–C13	1.933 (5)	C21–O21	1.134 (6)
Ru2–C21	1.924 (6)	C22–O22	1.130 (6)
Ru2–C22	1.936 (7)		

Table VII. Bond Angles (deg)

Ru1′–Ru1–Ru2	60.3 (1)	Ru1–Ru2–C21′	143.1 (2)
Ru1′–Ru1–N	47.5 (1)	Ru1–Ru2–C21	93.3 (2)
Ru1′–Ru1–C10	51.2 (2)	Ru1–Ru2–C22	122.2 (2)
Ru1′–Ru1–C11	93.8 (2)	N–Ru2–C10	82.0 (2)
Ru1′–Ru1–C12	147.6 (2)	N–Ru2–C21	96.4 (2)
Ru1′–Ru1–C13	118.6 (2)	N–Ru2–C22	166.2 (2)
Ru2–Ru1–N	46.4 (1)	C10–Ru2–C21	131.6 (2)
Ru2–Ru1–C10	49.8 (2)	C10–Ru2–C22	84.2 (3)
Ru2–Ru1–C11	144.9 (1)	C21–Ru2–C21′	96.8 (2)
Ru2–Ru1–C12	94.9 (1)	C21–Ru2–C22	92.7 (2)
Ru2–Ru1–C13	121.1 (2)	Ru1–N–Ru1′	85.0 (2)
N–Ru1–C10	80.6 (2)	Ru1–N–Ru2	86.5 (2)
N–Ru1–C11	98.9 (2)	Ru1–N–O	132.8 (2)
N–Ru1–C12	100.6 (2)	Ru2–N–O	117.6 (3)
N–Ru1–C13	163.0 (2)	Ru1–C10–Ru1′	77.5 (2)
C10–Ru1–C11	132.4 (2)	Ru1–C10–Ru2	79.1 (2)
C10–Ru1–C12	129.3 (2)	Ru1–C10–O10	133.4 (2)
C10–Ru1–C13	82.5 (2)	Ru1–C11–O11	178.3 (4)
C11–Ru1–C12	97.8 (2)	Ru1–C12–O12	176.8 (5)
C11–Ru1–C13	91.2 (2)	Ru1–C13–O13	177.6 (5)
C12–Ru1–C13	91.4 (2)	Ru2–C10–O10	132.3 (5)
Ru1′–Ru2–Ru1	59.5 (1)	Ru2–C21–O21	176.3 (5)
Ru1–Ru2–C10	51.1 (1)	Ru2–C22–O22	179.2 (7)
Ru1–Ru2–N	47.1 (1)	N–O–C	112.1 (5)

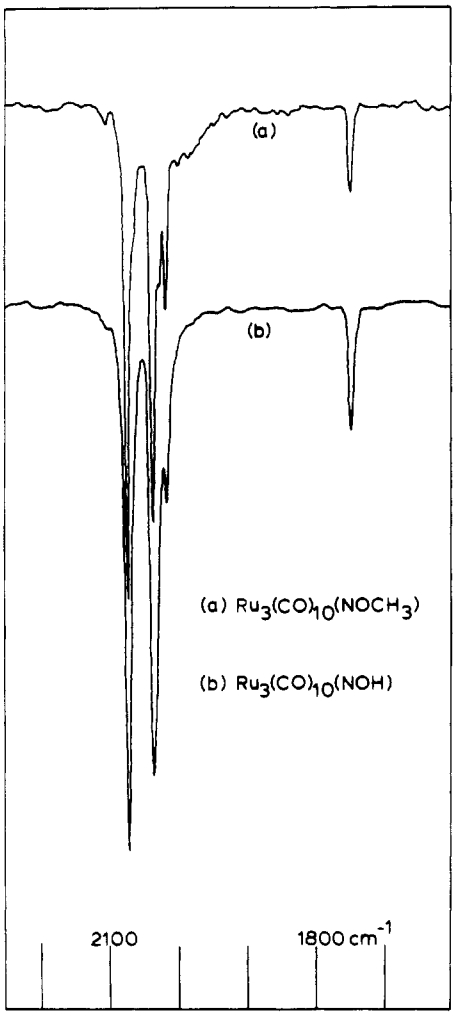

Figure 1. Infrared spectra in the carbonyl region for $Ru_3(NOCH_3)(CO)_{10}$ and $Ru_3(NOH)(CO)_{10}$. The solvent in both spectra is hexane.

in a reasonable position for one of the H atoms. Its position was not included in subsequent least-squares cycles. The values of atomic scattering factors were taken from the usual tabulation, and the effects of anomalous dispersion were included.[41] The positional parameters, bond distances, and angles are included in Tables V–VII, respectively.

Results

Synthesis and Characterization of $Ru_3(NOCH_3)(CO)_{10}$. Reaction of $PPN[Ru_3(CO)_{10}(NO)]$ with a stoichiometric amount of $CF_3SO_3CH_3$ in methylene chloride generates $Ru_3(NOCH_3)(CO)_{10}$ (eq 2). The bright lemon yellow air-stable product

$$PPN[Ru_3(CO)_{10}(NO)] + CF_3SO_3CH_3 \rightarrow Ru_3(NOCH_3)(CO)_{10} + PPN(CF_3SO_3) \quad (2)$$

can be isolated in 86% yield after chromatography with hexane. The infrared spectrum in hexane (Figure 1) shows the presence of a band of medium intensity at 1745 cm^{-1}, characteristic of a $M_3(\mu_3\text{-CO})$ group.[42] The infrared spectrum in a KBr pellet is similar and allowed the observation of a ν_{O-C} at 1040 (m) cm^{-1} and a ν_{N-O} at 945 (w) cm^{-1} ($\nu_{^{15}N-O}$ = 922 cm^{-1}). The ^{1}H NMR exhibits a singlet due to the methyl group that appears at 3.45 ppm ($CDCl_3$), which compares to the value of 4.56 ppm for the isoelectronic $HRu_3(COMe)(CO)_{10}$.[17,26] This singlet splits into a doublet when the compound is 90% enriched with ^{15}N. The ^{15}N NMR spectrum contains one resonance at 285.8 ppm (downfield from NH_3), which is 529 ppm upfield from the observed resonance of $[Ru_3(CO)_{10}(NO)]^-$.[11] This shift in the ^{15}N resonance in going from the μ_2-NO to the μ_3-$NOCH_3$ is substantially larger than the observed shift of the unique carbon resonance when $[HFe_3(CO)_{11}]^-$ is converted to $HFe_3(CO)_{10}(COCH_3)$.[21]

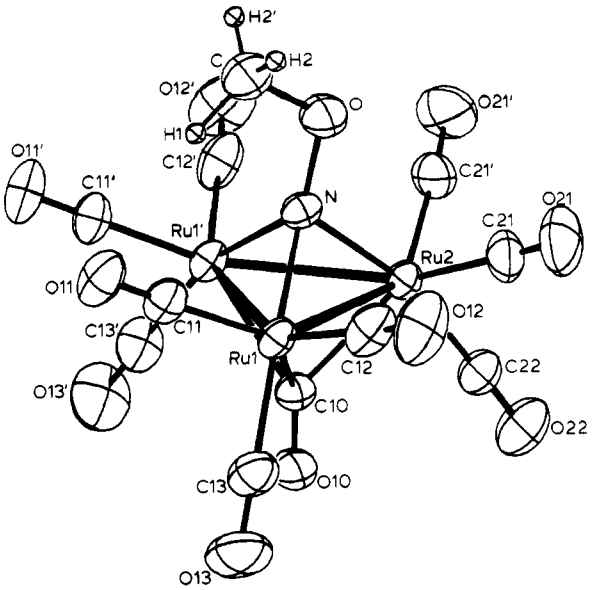

Figure 2. Structure of $Ru_3(NOCH_3)(CO)_{10}$ with the atom labels. The probability ellipsoids are indicated at the 50% level.

X-ray Crystallographic Analysis of $Ru_3(NOCH_3)(CO)_{10}$. In order to confirm that the reaction had indeed resulted in the O-methylation of the nitrosyl oxygen, a single-crystal X-ray analysis of the cluster was undertaken. The crystal structure consists of discrete molecules of $Ru_3(NOCH_3)(CO)_{10}$. No significant intermolecular interactions are observed. Figure 2 is a view of a single cluster showing the system used for labeling the atoms. Interatomic distances with their estimated standard deviations are listed in Table VI, and the interbond angles are shown in Table VII.

The cluster lies on a crystallographic mirror plane that passes through C–O–N–Ru2–C22–O22–C10–O10 giving the molecule C_s symmetry. Except for the methyl group, however, the molecular symmetry closely fits into the C_{3v} point group with a trigonal-bipyramidal core. Each metal atom has three terminal carbonyl ligands. The triangle of ruthenium atoms is triply bridged on one side by the unique carbonyl ligand (C10–O10) and on the other side by the methoxyimido ligand. The oxygen of this ligand is tilted toward Ru2, as measured by the Ru2–N–O angle of 117.6 (3)° compared to the Ru(1)–N–O angle of 132.8 (2)°.

The Ru1–Ru1′ and Ru1–Ru2 metal–metal vectors of lengths 2.740 (1) and 2.762 (1) Å, respectively, are significantly shorter than the average value of 2.854 (4) Å found for $Ru_3(CO)_{12}$.[43] This shortening of the metal–metal distances is undoubtedly due to the presence of the two triply bridging ligands. The average Ru–CO distance of 1.933 (9) Å, the average C–O distance of 1.13 (1) Å, and the average Ru–C–O angle of 177.6 (5)° all fall within the expected ranges, as does the C10–O10 distance of 1.175 (6) Å for the triply bridging carbonyl.

The methoxyimido ligand is bound to the triruthenium framework via the bonds Ru1–N = 2.027 (3) Å and Ru2–N = 2.006 (4) Å; the Ru1–N–Ru1′ angle is 85.0 (1)°, and the Ru1–N–Ru2 angle is 86.5 (2)°. The N–O bond distance is 1.433 (6) Å, and the O–C bond distance is 1.391 (8) Å. The N–O–C angle is 112.1 (5)°. The N–O distance is 0.04 Å longer than the reported distance for the N–O bond of the μ_3-NOH ligand in $[\eta^5\text{-}C_5H_4Me)_3Mn_3(NO)_3(NOH)]BF_4$.[34] However, in that structure the nitrosyl-bound hydrogen is hydrogen-bonded to the BF_4^- counterion, which allows for more multiple-bond character in the N–O bond. Both of the values are significantly longer than that

(41) (a) Cromer, D. T.; Waber, J. T. *International Tables for X-Ray Crystallography*; Kynoch Press: Birmingham, England, 1974; Vol. IV, Table 2.2A. Cromer, D. T. *Ibid.*, Table 2.3.1. (b) Cromer, D. T.; Ibers, J. A. *International Tables for X-Ray Crystallography*; Kynoch Press: Birmingham, England, 1974; Vol. IV, Table 2.2C.

(42) Smieja, J. A.; Gladfelter, W. L. *Inorg. Chem.* **1986**, *25*, 2667.

(43) Churchill, M. R.; Hollander, F. J.; Hutchinson, J. P. *Inorg. Chem.* **1977**, *16*, 2655.

Scheme I

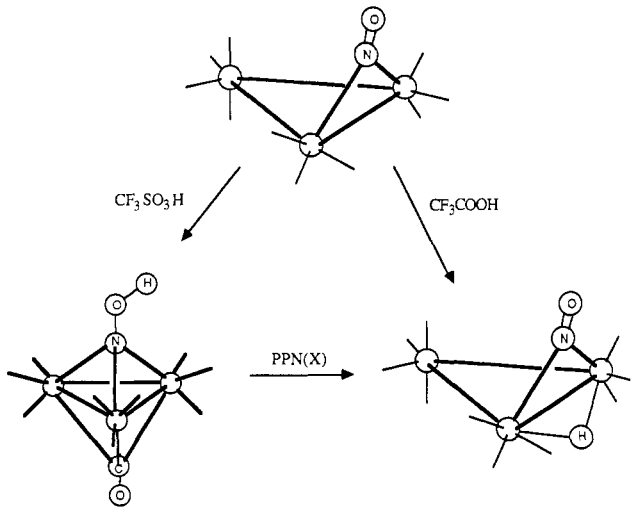

1

of the μ_3-NO ligand in $Cp_3Mn_3(NO)_4$, 1.247 (5) Å,[13] and that of the μ_2-NO of $[Os_3(CO)_{10}(NO)]^-$, 1.23 (1) Å.[12] The O–C distance is shorter than the observed distances for the O-methylated carbonyls of 1.467 (8) and 1.465 (10) Å for $HRu_3(CO)_{10}(COMe)$[25] and $PPN[Fe_4(CO)_{12}(COMe)]$,[44] respectively. The N–O–C angle is between the C–O–C angles of 119.42 (44) and 117.3 (6)° of $HRu_3(CO)_{10}(COMe)$[25] and $PPN[Fe_4(CO)_{12}(COMe)]$[44] and the N–O–H angle of 107 (4)° for $[Cp_3Mn_3(NO)_3(NOH)]BF_4$.[34]

The overall structure of $Ru_3(NOMe)(CO)_{10}$ is similar to those of other $Ru_3(NR)(CO)_{10}$ species such as $Ru_3(NPh)(CO)_{10}$[45] and $FeRu_2(NH)(CO)_9[P(OCH_3)_3]$.[46] An interesting comparison is that between this structure and the isoelectronic $HM_3(COMe)(CO)_{10}$ species, M = Fe[14] and Ru.[25] These complexes contain doubly bridging COMe and hydride ligands. However, it has been noted[14] that both the COMe ligand and a carbonyl ligand on the unique metal atom are semitriply bridging, making the structure similar to that of $Ru_3(NOMe)(CO)_{10}$. In recent studies involving heteronuclear clusters, such as $HCoFe_2(Cp)(CO)_7(COMe)$, the methoxymethylidyne ligand was found in the triply bridging position.[30]

Synthesis and Characterization of $Ru_3(NOH)(CO)_{10}$. If CF_3SO_3H is used in place of $CF_3SO_3CH_3$, an O-protonated complex, $Ru_3(CO)_{10}(NOH)$, is produced (eq 3). The bright

$$PPN[Ru_3(CO)_{10}(NO)] + CF_3SO_3H \rightarrow Ru_3(NOH)(CO)_{10} + PPN(CF_3SO_3) \quad (3)$$

lemon yellow species cannot be isolated by chromatography and can only be obtained as an unstable dark yellow oil. The infrared spectrum of this cluster in hexane is virtually superimposable on that of $Ru_3(NOMe)(CO)_{10}$ (Figure 1). A weak absorbance at 3495 cm^{-1} (CH_2Cl_2) is assigned to the ν_{O-H}, and the ν_{N-O} is observed at 1110 cm^{-1} ($\nu_{^{15}N-O}$ = 1090 cm^{-1}), which compares well with the observed ν_{N-O} of $Ru_3(NOMe)(CO)_{10}$. The ^1H NMR spectrum exhibits a singlet due to the hydroxyimido ligand at 8.90 ppm ($CDCl_3$). This value compares to 16.1 and 15.0 ppm for the μ_2-COH ligand in $HRu_3(COH)(CO)_{10}$[23,27] and $HFe_3(COH)(CO)_{10}$,[21] respectively. The μ_3-COH ligand in $Co_3(COH)(CO)_9$[22] and μ_4-COH in $HFe_4(COH)(CO)_{12}$[24] have proton resonances at 11.25 and 13.2 ppm, respectively. No resonance assignable to the O-protonated nitrosyl in $[Cp_3Mn_3(NO)_3(NOH)]BF_4$ was found, a phenomenon attributed to the hydrogen bonding of this species.[34]

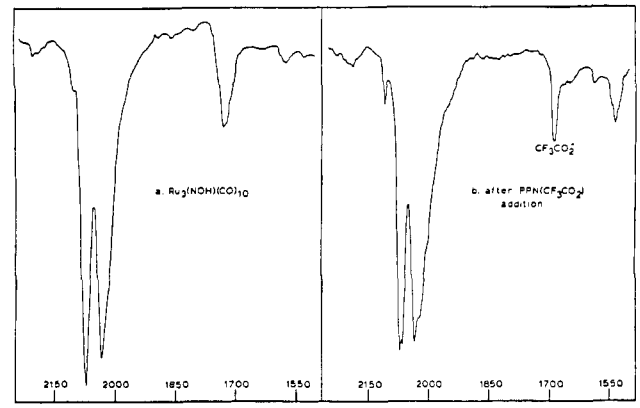

Figure 3. Infrared spectra of a tautomerization experiment: (a) $Ru_3(NOH)(CO)_{10}$ in CH_2Cl_2; (b) same solution immediately following the addition of $PPN(CF_3CO_2)$ in CH_2Cl_2.

The ^{15}N NMR spectrum of $Ru_3(NOH)(CO)_{10}$ exhibits a resonance at 250.6 ppm, which is very similar to the chemical shift of the methoxyimido nitrogen of $Ru_3(NOMe)(CO)_{10}$. In contrast, the chemical shift of the nitrogen in $HRu_3(CO)_{10}(NO)$ is 807.7 ppm.[11] Again, the shift in the nitrogen resonance in going from μ_2-NO to μ_3-NOH is substantially larger than that observed for the unique carbon resonance when $[HFe_4(CO)_{13}]^-$ is converted to $HFe_4(COH)(CO)_{12}$.[24] However, in contrast to the carbon system, the μ_3-NOMe resonance is further downfield than that of the μ_3-NOH group. The spectroscopic similarities between $Ru_3(NOMe)(CO)_{10}$ and $Ru_3(NOH)(CO)_{10}$ allow the assignment of struture **1** (Scheme I) to the O-protonated cluster. The surprising feature about $Ru_3(NOH)(CO)_{10}$ is not so much that it forms, but that it is remarkably stable compared to its carbonyl analogues. At room temperature, a CH_2Cl_2 solution of $Ru_3(NOH)(CO)_{10}$ shows no conversion to $HRu_3(CO)_{10}(NO)$ or any other product for hours. The cluster will decompose in hexane solution at any temperature over a period of days to non-carbonyl-containing materials. In contrast, the O-protonated carbonyl, $HRu_3(COH)(CO)_{10}$, readily converts to $H_2Ru_3(CO)_{11}$ above −30 °C.[23,27]

It was discovered that addition of certain anions to solutions of $Ru_3(NOH)(CO)_{10}$ caused immediate conversion to $HRu_3(CO)_{10}(NO)$. Figure 3 illustrates the infrared spectral changes that accompany the tautomerization affected by the addition of $PPN(CF_3SO_3)$. Workup of the reaction allows the isolation of $HRu_3(CO)_{10}(NO)$ in 79% overall yield from $PPN[Ru_3(CO)_{10}(NO)]$.

Substituted Analogues. The substituted analogues, $[Ru_3(CO)_9L(NO)]^-$, also exhibit site-selective protonation and anion-assisted tautomerization (eq 4 and 5). The hydroxyimido species

$$[Ru_3(CO)_9L(NO)]^- + CF_3SO_3H \rightarrow Ru_3(NOH)(CO)_9L + CF_3SO_3^- \quad (4)$$

$$Ru_3(NOH)(CO)_9L + CF_3CO_2^- \rightarrow HRu_3(CO)_9L(NO) + CF_3CO_2^- \quad (5)$$

2a, L = $P(OCH_3)_3$
2b, L = PPh_3
3a, L = $P(OCH_3)_3$
3b, L = PPh_3

have not been isolated, but they have been characterized spectroscopically (Table I). The infrared spectrum of **2a** in hexane is similar to that of $Ru_3(NOH)(CO)_{10}$, with a lowering of the energy of the carbonyl stretches due to the presence of the phosphite ligand. **2b** is not soluble in hexane, but its spectrum in CH_2Cl_2 is superimposable on that of **2a**. The O–H proton has a resonance at 9.32 and 8.80 ppm for **2a** and **2b**, respectively. These values compare well with the 8.90 ppm chemical shift for the O–H proton in the unsubstituted material. Interestingly, the chemical shift of the phosphorus changes much less upon O-protonation ($\Delta\delta$ = −11.6 ppm for **2a**; $\Delta\delta$ = −3.6 ppm for **2b**) than it does upon protonation of the metal–metal bond ($\Delta\delta$ = 23.0 ppm, L = $P(OCH_3)_3$; $\Delta\delta$ = 15.8 ppm, L = PPh_3).

(44) Holt, E. M.; Whitmire, K. H.; Shriver, D. F. *J. Am. Chem. Soc.* **1982**, *104*, 5621.
(45) Bhaduri, S.; Gopalkrishnan, K. S.; Sheldrick, G. M.; Clegg, W.; Stalke, D. *J. Chem. Soc., Dalton Trans.* **1983**, 2339.
(46) Blohm, M. L.; Fjare, D. E.; Gladfelter, W. L. *J. Am. Chem. Soc.* **1986**, *108*, 2301.

2a and **2b** are tautomerized to **3a** and **3b**, respectively, with $CF_3CO_2^-$. **2b**, in fact, is the initial product upon protonation with CF_3CO_2H. **3b** then is slowly formed over a 3-h period.

Discussion

It is somewhat surprising that there is such complete selectivity for two different sites of protonation using two different strong acids (Scheme I). It has previously been shown that protonation of $PPN[Ru_3(CO)_{10}(NO)]$ with CF_3CO_2H in methylene chloride gives $HRu_3(CO)_{10}(NO)$.[11] But as discussed earlier, protonation under identical conditions with CF_3SO_3H gives $Ru_3(NOH)(CO)_{10}$. The major difference between CF_3CO_2H and CF_3SO_3H is the much higher acidity of CF_3SO_3H ($H_0 = -13$)[47] compared to CF_3CO_2H ($H_0 = -2.77$).[48] O-Protonation with CF_3CO_2H may simply be thermodynamically unfavorable, which can easily explain the observed selectivity. This statement would require that $Ru_3(NOH)(CO)_{10}$ be a stronger acid than $HRu_3(CO)_{10}(NO)$, which is proven below. The selectivity displayed by CF_3SO_3H must then be related to a higher kinetic barrier for M-protonation compared to O-protonation. There is ample evidence from detailed studies indicating that rates of proton transfer involving M–H groups are slow compared to those involving O–H or N–H groups.[49,50]

The anion-assisted O–H to M–H tautomerization found in this system demonstrates the difference between the kinetic site of protonation (the nitrosyl oxygen) and the thermodynamic site of protonation (the metal–metal bond). The results can be understood in terms of the two equilibria (6) and (7). The kinetic site

$$Ru_3(NOH)(CO)_{10} + X^- \underset{k_{-1}}{\overset{k_1}{\rightleftharpoons}} HX + [Ru_3(CO)_{10}(NO)]^- \quad (6)$$

$$HX + [Ru_3(CO)_{10}(NO)]^- \underset{k_{-2}}{\overset{k_2}{\rightleftharpoons}} HRu_3(CO)_{10}(NO) + X^- \quad (7)$$

of protonation being the nitrosyl oxygen means simply that $k_{-1} \gg k_2$. Thermodynamically, however, in order for $HRu_3(CO)_{10}(NO)$ to be the product, $K_2(k_2/k_{-2})$ must be greater than $K_1^{-1}(k_{-1}/k_1)$. After the preparation of $Ru_3(NOH)(CO)_{10}$ and addition of X^-, the tautomerization can occur if and only if X^- is a strong enough base to deprotonate the (NOH) species.

Table III shows the results of tautomerization experiments with a series of PPN^+ salts of strong acids. For illustrative purposes only, the corresponding pK_a values of the strong acids in acetonitrile are also listed.[51-53] The dissociation constants of strong acids in halogenated hydrocarbon solvents have not been measured due to their low dielectric constants ($D < 10$) and dipole moments (<2 D).[52] In fact, only one report of such a dissociation constant has appeared in the literature, where Nae and Jagur-Grodzinski estimated the pK_a of picric acid in 1,2-dichloroethane to be ~ 11.[54] In the absence of quantitative data for a pH scale in methylene chloride, only qualitative conclusions can be drawn from these experiments. For the weakest bases, X^- is not sufficiently strong to drive eq 6 to the right, which implies that $k_{-1} \gg k_1$, and tautomerization does not occur. In an attempt to drive eq 6 to the right, a 10-fold excess of $PPN(FSO_3)$ was added to a CH_2Cl_2 solution of $Ru_3(NOH)(CO)_{10}$ to disturb the equilibrium. Even with the excess anion, no tautomerization was observed. For the stronger bases, addition of X^- drives eq 6 to the right, but HX is still a strong enough acid to protonate the metal–metal bond and also drive eq 7 to the right. This result shows that, no matter what the individual rates of k_1, k_{-1}, k_2, and k_{-2} are, K_2 is much greater than K_1. Therefore, from the results of the tautomerization reactions and the relative strengths of the acids in acetonitrile, it can be shown that $Ru_3(NOH)(CO)_{10}$ is a weaker acid than $HFSO_3$ but a stronger acid than HBr.

The tautomerization for the substituted materials is much slower than for $Ru_3(NOH)(CO)_{10}$. The relative rates of tautomerization are $CO \gg P(OCH_3)_3 > PPh_3$. This is the same order as both the π-accepting ability and the size of the ligands, so it is not possible to discern whether the observed effect is electronic or steric in nature.

Acknowledgment. This research was funded by a grant from the National Science Foundation.

Supplementary Material Available: Listings of complete crystal data and temperature factors (2 pages); tables of calculated and observed structure factors (7 pages). Ordering information is given on any current masthead page.

(47) Howells, R. D.; McCown, J. D. *Chem. Rev.* **1977**, *77*, 69.
(48) Eaborn, C.; Jackson, P. M.; Taylor, R. *J. Chem. Soc. B* **1966**, 613.
(49) Edidin, R. T.; Sullivan, J. M.; Norton, J. R. *J. Am. Chem. Soc.* **1987**, *109*, 3945.
(50) Walker, H. W.; Pearson, R. G.; Ford, P. C. *J. Am. Chem. Soc.* **1983**, *105*, 1179.
(51) Fujinaga, T.; Sakamoto, I. *J. Electroanal. Chem. Interfacial Electrochem.* **1977**, *85*, 185.
(52) Kolthoff, I. M.; Chantooni, M. K., Jr. In *Treatise on Analytical Chemistry*; Kolthoff, I. M.; Elving, P. J., Eds.; Wiley: New York, 1979; Part I, Vol. 2, p 239.
(53) Kolthoff, I. M.; Wang, W.-J.; Chantooni, M. K., Jr. *Anal. Chem.* **1983**, *55*, 1202.
(54) Nae, N.; Jagur-Grodzinski, J. *J. Am. Chem. Soc.* **1977**, *99*, 489.